

UNCERTAINTY QUANTIFICATION AND ROBUST OPTIMIZATION FOR THROUGHFLOW AXIAL COMPRESSOR DESIGN

J. Sans - T. Verstraete - J.-F. Brouckaert

Turbomachinery and Propulsion Department, Von Karman Institute for Fluid Dynamics
72, Chaussée de Waterloo, B-1640 Rhode-Saint-Genèse Belgium,
sans@vki.ac.be

ABSTRACT

Throughflow axial compressor design relies on empirical correlations to estimate the total pressure losses and deviation generated by a blade row. Those correlation data have been obtained with given measurement uncertainties that are usually not taken into account by meridional design tools or throughflow solvers. Uncertainty quantification techniques such as Monte-Carlo sampling or stochastic collocation can help to introduce uncertainties within those numerical tools and quantify their effects on the compressor performance at cheap computational costs. The throughflow solver used for this investigation is ACPreDesign. The code has been recently implemented at VKI and solves the non-isentropic radial equilibrium equations for axial compressors. Realistic uncertainties are introduced from standard loss correlations. The implementation of non-intrusive uncertainty quantification methods is presented and validated on a single stage low pressure compressor geometry studied at VKI. The results are analyzed in terms of efficiency probability density functions which represent the resulting uncertainties on efficiency due to non-deterministic loss correlations. Finally, ACPreDesign is coupled to the VKI optimizer CADO in order to approach the problem of design under uncertainty also referred to as robust design. To address that issue the paper focuses on a robust solidity optimization of a single rotor configuration.

NOMENCLATURE

D	Diffusion factor	[-]	CFD	Computational Fluid Dynamics
H_n	n -order Hermite's polynomial	[-]	IGV	Inlet Guide Vane
U	uncertain input	[]	NISRE	Non-Isentropic Radial Equilibrium
ζ	Loss parameter	[-]	PDF	Probability Density Function
β_2	Outlet flow angle	[°]	UQ	Uncertainty Quantification
η	Efficiency	[-]	VKI	von Karman Institute for Fluid Dynamics
μ	Average	[]		
ξ	Random variable	[]		
σ	Solidity	[-]		
	or Standard deviation	[]		
ω	Total pressure loss	[-]		

INTRODUCTION

The meridional design is an essential step in the elaboration of any turbomachinery component. Many choices, such as the channel geometry or the solidity, are done at the level of the meridional design and may influence the rest of the whole design process.

However, any radial equilibrium solver relies on empirical correlations. Those correlations provide an estimate of the total pressure losses of a blade row depending on its loading and number of blades. For compressors, such correlations originally come from the work of Lieblein et al. (1953) but have been completed to provide spanwise corrections like in the work of Robbins et al. (1965). Nevertheless, it must not be forgotten that all empirical correlation data have been obtained within given measurement uncertainty bands. Similarly, many correlations often present a big scatter in the data due to the wide variety of tested profiles and a polynomial curve fit is usually drawn through the measurement points to allow for an implementation in a throughflow solver. The uncertainties or the data scatter is then neglected.

Since nowadays meridional calculations are very cheap in terms of computational time, it is very appealing to combine throughflow solvers with optimizer tools and/or with uncertainty quantification (UQ) techniques which both require many evaluations such as evolutionary algorithms or Monte-Carlo sampling and stochastic collocation techniques.

The main purpose of UQ methods is to improve the confidence in any numerical prediction by considering a probabilistic framework and epistemic uncertainties. These are defined as a potential defect or deficiency due to a lack of knowledge. They may be seen as model uncertainties. As an example, the geometrical variability with respect to the theoretical design that may appear during the manufacturing or because of some damages occurring during the engine life cycle may be seen as a source of epistemic uncertainties. Those are usually disregarded, especially at the early phase of the meridional design. Nonetheless, the impact of those geometrical variabilities at the level of the throughflow design have been studied by Lecerf et al. (2003) or Panizza et al. (2014) respectively for high-pressure compressors and centrifugal compressors. In any CFD computations, the turbulence models are another important source of epistemic uncertainties that are not taken into account by deterministic approaches. Similarly, the uncertainties related to any loss or deviation empirical correlations in a meridional solver are most of the time neglected and the originality of the current investigation resides in the consideration of the epistemic uncertainties of such empirical models by the means of UQ methods.

The use of UQ techniques and how they are implemented into a design process is the main focus of the current paper. To illustrate the methods, the emphasis is set on the solidity optimization of a given compressor geometry. After briefly presenting the compressor geometry and the solver, the results of solidity optimization without UQ are firstly given. Based on those optimum designs, UQ is introduced by using both sampling or quadrature methods. The loss correlations are parametrized to analyze their impact on the results. The last issue addressed in the paper is the problem of optimization under uncertainty commonly referred to as *robust design*. The results are discussed with and without the use of UQ.

AXIAL COMPRESSOR PRE-DESIGN TOOL

The meridional solver that is used is *ACPreDesign*. This multi-stage axial compressor design program originally comes from Creveling and Carmody (1968) and has been recently implemented at VKI. It solves the non-isentropic radial equilibrium equations for given design input parameters. Currently, the program does not provide off-design predictions. Examples of meridional optimization using *ACPreDesign* can be found in the work of Joly et al. (2012) or Teichel et al. (2013).

The compressor flowpath geometry must be imposed and divided into a number of axial stations where the radial equilibrium equations will be solved. The mass flow, the inlet total pressure and temperature, the desired global mass-averaged pressure ratio and the rotating speed of every stage must be provided. If the flow does not enter the rotor axially, the rotor inlet tangential velocity distribution can be modeled by an IGV row. For each stage, outlet tangential velocity distributions (at both rotor and stator outlets) as well as both rotor and stator solidity distributions are also required.

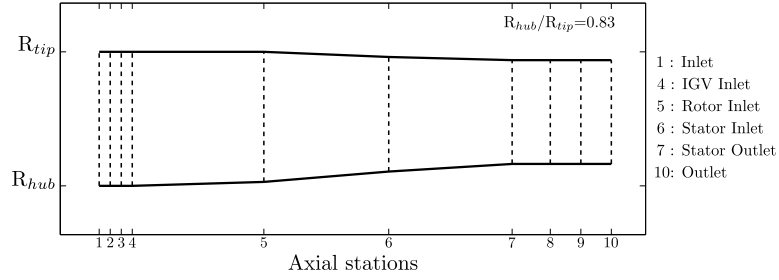


Figure 1: Channel and axial station locations

The channel geometry and the axial stations are sketched in Fig. 1. The flowpath coordinates are coming from a low-pressure compressor studied both numerically and experimentally at VKI (Sans et al., 2013). An IGV row has been set in front of the rotor in order to match the desired inlet tangential velocity distribution. All tangential velocity profiles as well as the nominal RPM and design mass-flow have been imposed following the original design specifications.

In order to compute the total pressure losses of each row, ACPReDesign relies on loss correlations originally coming from the work of Lieblein et al. (1953), presented in Fig. 2.

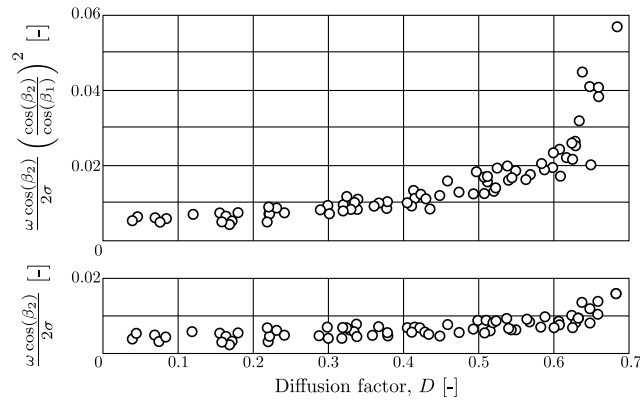


Figure 2: Loss correlations of Lieblein et al. (1953)

The correlations implemented by Creveling and Carmody are based on the work of Robbins et al. (1965) and include three-dimensional corrections to have a realistic spanwise loss evolution. Rotor correlation curves are available in Fig. 3. They are given in terms of diffusion factor versus a loss parameter ζ (like in Fig. 2) defined by Eq. 1 that is depending on the total pressure losses ω , the outlet flow angle β_2 and the solidity σ .

$$\zeta = \frac{\omega \cos(\beta_2)}{2\sigma} \quad (1)$$

The mid-span rotor loss evolution is the lowest as it only contains profile losses. The hub curve is shifted to a higher loss level to account for secondary flows and potentially corner vortex separation. The tip losses are equal to the mid-span losses until a diffusion factor of 0.40 which triggers the growth of losses due to the tip gap vortex.

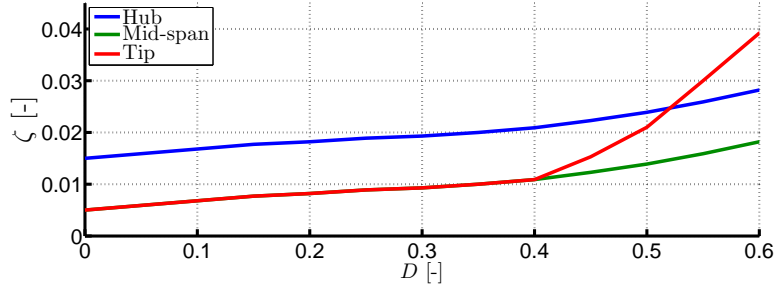


Figure 3: Rotor loss correlations of ACPreDesign

From the comparison of Fig. 2 and Fig. 3, it clearly emerges that the scatter of Fig. 2 has not been implemented in the correlations of ACPreDesign. This is a typical example of an epistemic uncertainty.

OPTIMIZATION

Method and constraints

ACPreDesign has been coupled to the VKI optimizer CADO (Verstraete, 2010) to find the best solidity distributions in terms of efficiency for a given pressure ratio distribution. The solidity is imposed at three span locations (10%, 50% and 90%) and a 2nd order Bezier interpolation is used to compute the solidity distribution. More than simply the global average pressure ratio, the whole pressure ratio spanwise distribution may be imposed. It is controlled through the rotor outlet tangential velocity distribution which is optimized together with the solidity distribution to satisfy the design requirements both in terms of spanwise pressure ratio distribution and global average pressure ratio.

The VKI optimization code CADO is based on a differential evolution (DE) algorithm. This evolutionary method has been developed by Price and Storn (1997). Originally implemented for axial turbomachinery blade optimization, CADO has since then been improved and extended to multidisciplinary optimizations by Verstraete (2008). The algorithm can easily be coupled to any solver as in the present case to ACPreDesign. As mentioned earlier, the previous work of Joly et al. (2012) or Teichel et al. (2013) are very good examples of ACPreDesign optimizations using CADO. The major drawback of DE is that it requires a large number of evaluations which, in some situations, may become unrealistic depending on the complexity of the optimization problem and the solver. The use of metamodels may help to reduce the total computational cost but, in the case of ACPreDesign, the number of evaluations does not represent an issue.

Various constraints may be imposed by the designer. They may be set on aerodynamic performance parameters (maximum turning of the airfoil, diffusion factor etc...) or involve mechanical considerations (maximum RPM). In the current situation, the most limiting parameter is the maximum diffusion factor which has been constrained over the whole span. This parameter has a big influence on the results of the optimization. A constraint has been set on the pressure ratio at an arbitrary level of 1.25. The problem becomes a single-objective optimization since only the efficiency is maximized. The solidity is directly linked to the spanwise distribution of the chord length which may be subjected to various mechanical additional constraints. Consequently, the solidity profile is not

completely arbitrary. Although no chord length limitation has been considered in the current paper, it must be mentioned that it is also possible to add specific constraints on the solidity or the chord as well as on their slope or curvature. This can fasten the whole design process by taking into account some mechanical requirements of the latest design phase at the early stage of the throughflow design.

Optimum solidity distributions

The constraint on the diffusion factor has quickly been identified as a crucial parameter. Optimizations have been run varying the maximum rotor diffusion factor D_{max} from 0.375 to 0.45 by steps of 0.025 as well as for $D_{max} = 0.50$. Optimizations have also been run on the full stage but only the single rotor configuration results are presented in the paper.

The rotor optimum solidity distributions are displayed in Fig. 4 next to the corresponding diffusion factor distributions in Fig. 5. Increasing D_{max} , the mean solidity decreases. The trend of solidity versus span becomes linear for $D_{max} = 0.425$ and then changes curvature for higher diffusion. For $D_{max} > 0.425$, the tip solidity remains around 0.9. Looking at the corresponding diffusion factors, it seems that, for $D_{max} \leq 0.425$, the diffusion factor is higher at the hub than at the tip. More precisely, the diffusion level remains around 0.40 in the tip section. It underlines that an optimum diffusion lies around 0.40 at the tip but does not remain optimal towards the hub sections.

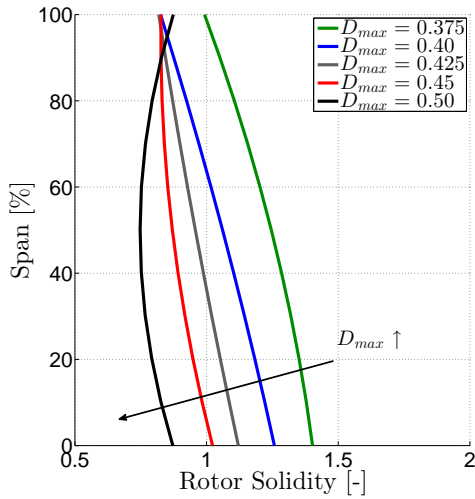


Figure 4: Optimum rotor solidity distributions for different values of D_{max}

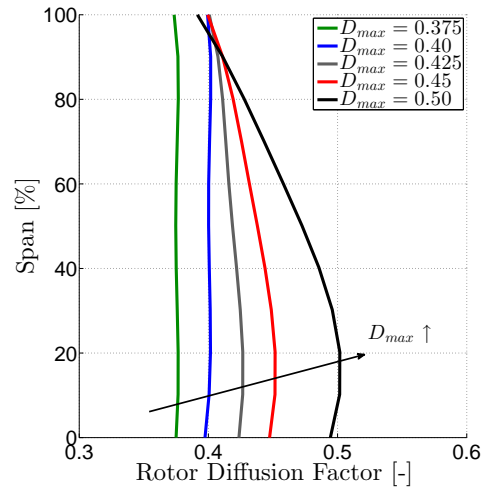


Figure 5: Rotor diffusion factor distributions for different values of D_{max}

The rotor efficiency distributions in Fig. 6 show that higher efficiency is obtained with increasing D_{max} . While the hub and mid-span efficiencies always increase for higher D_{max} , at the tip, the efficiency remains constant for $D_{max} > 0.40$. It can also be noticed that for each value of D_{max} , the highest efficiency is achieved at mid-span since the correlation curves of Fig. 3 always give the lowest amount of losses at mid-span. The highest efficiency is achieved with $D_{max} = 0.50$ which is obviously a very theoretical result since a rotor enduring a diffusion factor of 0.50 at design would most probably have no stall margin. However, as mentioned earlier, off-design predictions are not yet available in ACPredesign.

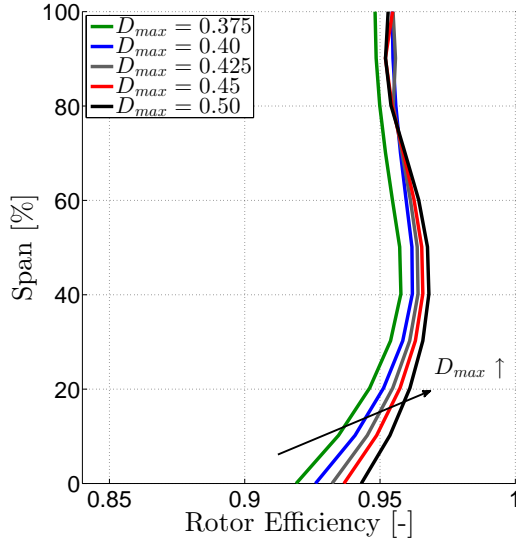


Figure 6: Rotor efficiency distributions for different values of D_{max}

UNCERTAINTY QUANTIFICATION

The previous section revealed that the loss correlations play an important role in the determination of an optimum solidity. The correlations affect the prediction of efficiency and the existence of an optimum diffusion (and solidity). In that prospect, looking back at the correlation data of Lieblein et al. in Fig. 2, a big scatter is observed in the data points. This source of uncertainty can be taken into account by the use of uncertainty quantification techniques.

The main idea of such methods is to improve the confidence in the predictions of ACPreDesign by adopting a non-deterministic approach. Within that probabilistic framework, an input vector $X = (x_1, x_2, \dots, x_D)$ and an output $y = g(X)$ are considered. The input vector X is an independent random variable corresponding to a given sample space and the output variable y is a stochastic quantity. The function g is the solver ACPreDesign in the current investigation but could possibly be any complex fluid dynamics model or CFD tool. The objective is to compute the output probability density function (PDF) f_y in order to compute its statistics, as the expected value $\mathbb{E}[y]$ and the variance $Var[y]$ given in Eq. 2 and Eq. 3.

$$\mathbb{E}[y] = \int_{-\infty}^{+\infty} z f_y(z) dz \quad (2)$$

$$Var[y] = \int_{-\infty}^{+\infty} (z - \mathbb{E}[y])^2 f_y(z) dz = \mathbb{E}[y^2] - (\mathbb{E}[y])^2 \quad (3)$$

Different methods exist in order to include uncertainties within the numerical predictions. They are characterized by their *intrusive* or *non-intrusive* nature. The method is considered as intrusive if the deterministic mathematical formulation (i.e. the source code) of the problem must be modified. Those methods have not been considered. On the opposite, sampling and quadrature methods are non-intrusive. Both are briefly presented below but more details about UQ methods in general are given by Iaccarino (2011).

Sampling techniques are the simplest approaches to propagate uncertainties. They rely on repeated simulations with different values of the input variables to generate the statistics of the output popula-

tion. The most famous sampling approach is the Monte-Carlo method. As mentioned by Iaccarino, the strength of sampling resides in the fact that it is universally applicable and will always converge to the exact stochastic solution if the number of samples tends to the infinity. The main drawback of Monte-Carlo sampling is that the convergence is very slow as, to build the statistics, it requires a large number of realizations.

Stochastic collocation refers to quadrature methods used to compute the statistics of random variables. Such methods enables to calculate the integrals (such as Eq. 2 and Eq. 3) from a discrete (preferably low) number of realizations. The Gauss-Hermite quadrature is often used in the field of uncertainty quantification. For random variables described by normal distribution, the formulation of the n -points quadrature is:

$$\int_{-\infty}^{+\infty} y(\xi) e^{-\xi^2} d\xi \approx \sum_{i=0}^n w_i y(\xi_i) \quad (4)$$

where ξ_i are the roots of the Hermite polynomials $H_n(x)$ and w_i are weights to which the Hermite polynomials are also associated. The weight w_i is defined as,

$$w_i = \frac{2^{n-1} n! \sqrt{\pi}}{n^2 [H_{n-1}(\xi_i)]^2}. \quad (5)$$

Having $H_0(x) = 1$ and $H_1(x) = 2x$, Hermite polynomials are linked through the following recurrence relation:

$$H_{n+1} = 2xH_n(x) - 2nH_{n-1}(x). \quad (6)$$

Parametrization

The rotor loss have been parametrized with three uncertain parameters. The first parameter U_{mean} shifts the mean loss level of hub, mid-span and tip correlation curves. For a given value of diffusion factor D , the rotor loss parameter is an independent normally distributed random variable of mean μ and variance σ . The mean μ is given by the default evolution of ACPReDesign of the rotor loss parameter versus diffusion factor, i.e. $\mu = \zeta(D)$. The variance of U_{mean} is constant over the whole span and diffusion range and comes from the analysis of Fig. 2. Assuming that the data observed in Fig. 2 corresponds to 95% of the individuals, it can be stated that the scatter is equal to $2 * 1.96 * \sigma = 3.92 \sigma$. Finally, observing that the scatter is about 0.005 at constant diffusion, the variance σ is equal to $1.275 * 10^{-3}$. This parameter simply shifts the loss curves to higher or lower levels. For the hub and mid-span loss curves, U_{mean} is the only uncertainty and both curves are just translated.

For the tip correlation curve, another parameter, noted U_D , controls the value of the diffusion factor where the losses start to rise. The last parameter U_{stall} introduces additional uncertainty on the losses at stall, i.e. at $D = 0.6$. By changing U_{stall} independently from U_{mean} and U_D , the slope of the tip loss curve between the diffusion factor given by U_D and $D = 0.6$ is varying. The situation is illustrated in Fig. 7 showing the three uncertain parameters U_{mean} , U_D and U_{stall} .

The choice of the mean and variance of U_D and U_{stall} is more arbitrary. The variance of U_{stall} has been set to two times the variance of U_{mean} (i.e., $\sigma_{U_{stall}} = 2 * 1.275 * 10^{-3}$). For U_D , a mean diffusion factor of 0.4 and a variance of 0.01 have been considered. Those values are summarized in Table 1.

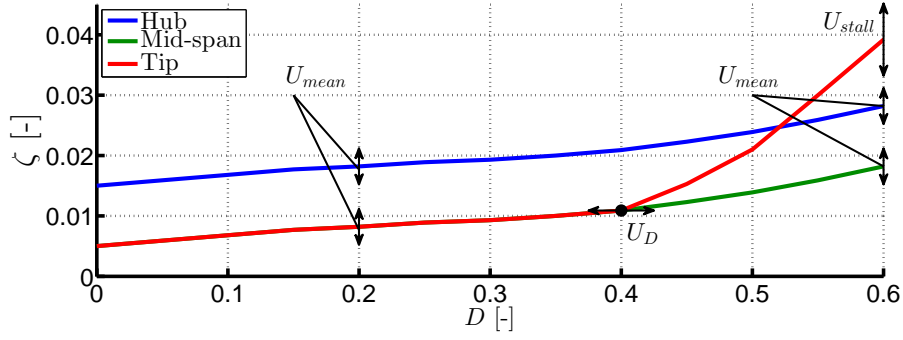


Figure 7: Rotor loss parametrization with three uncertain variables U_{mean} , U_D and U_{stall}

	μ [-]	σ [-]
U_{mean}	$\zeta_R(D)$	$1.275 \cdot 10^{-3}$
U_D	0.40	0.01
U_{stall}	$\zeta_R(D = 0.6)$	$2.55 \cdot 10^{-3}$

Table 1: Mean and variance of the three uncertain parameters U_{mean} , U_D and U_{stall}

Results

Considering the optimum solidity distribution of the previous section at $D_{max} = 0.45$, U_{mean} , U_D and U_{stall} have been randomly sampled 35.000 times although a minimum of 10.000 samples is usually sufficient. After 35.000 computations of ACPreDesign, the statistics of this population have been analyzed in terms of pressure ratio and efficiency. Both Fig. 8 and Fig. 9 illustrate the convergence of the efficiency mean and standard deviation. The minimum amount of samples is very case sensitive and depends on the order of statistics that is required. In the current case, 20.000 appeared sufficient since both the mean and the standard deviation do not significantly change above 20.000 samples.

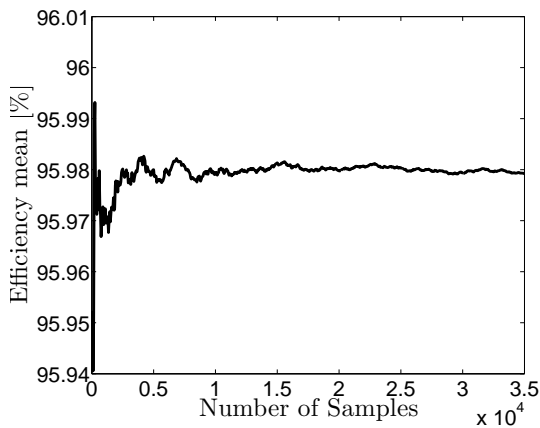


Figure 8: Evolution of the efficiency mean with the number of samples ($D_{max} = 0.45$)

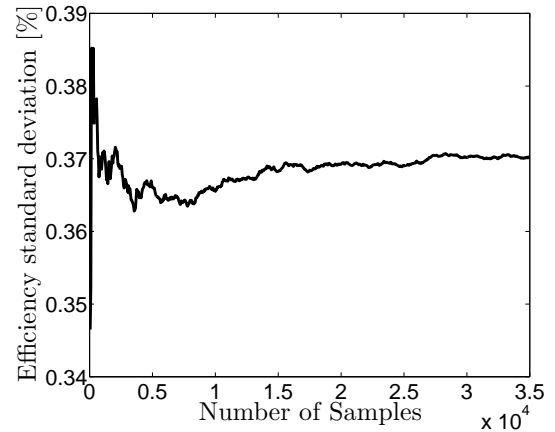


Figure 9: Evolution of the efficiency standard deviation with the number of samples ($D_{max} = 0.45$)

Before stochastic collocations may be applied, the user must know the nature of the output PDF. Indeed, depending on the kind of output PDF, different quadrature methods exist. Although Monte-Carlo sampling is very time and resource consuming, it remains the only way to characterize almost continuously the output PDF. To ensure a PDF is following a normal distribution, the population is presented in a histogram as well as in a probability plot. To build such a plot, based on the resulting mean μ and standard deviation σ , a theoretical normal distribution $N(\mu, \sigma)$ is plotted against the obtained population that has been formerly sorted in ascending order. If the population is normally distributed, the plot must look as a straight line. The histogram and the probability plot are shown in Fig. 10 which clearly proves the efficiency is normally distributed. The histogram in Fig. 10 also gives a very good image of the scatter induced by non-deterministic loss correlations on the efficiency. Depending on the required confidence interval, the width approaches 1.5%.

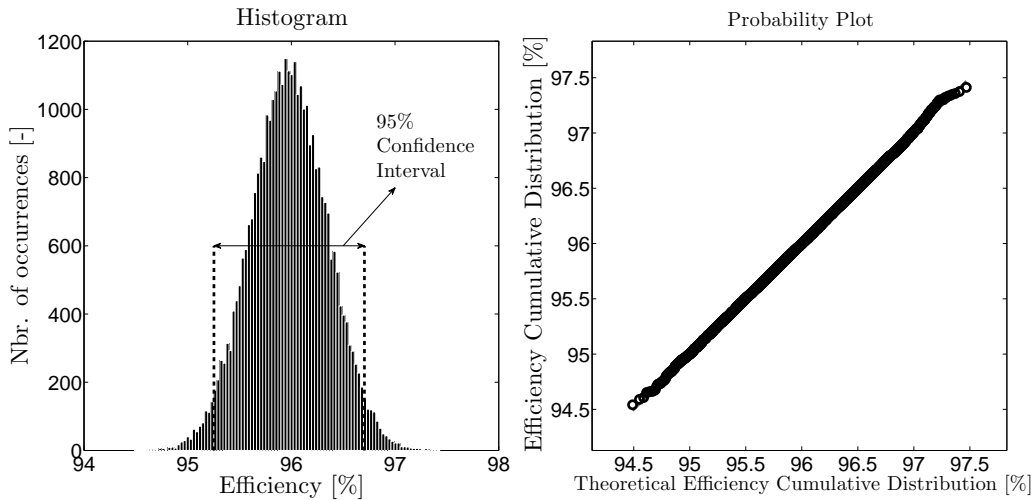


Figure 10: Efficiency histogram and probability plot ($D_{max} = 0.45$)

Given that the output PDF is Gaussian, the Hermite's quadrature may be used to perform stochastic collocation. Quadratures using 2, 3 and 4 points have been applied. Since there are three uncertain parameters, ACPreDesign must be run 8, 27 or 81 times in order to generate the output statistics. Results of stochastic collocations are compared to Monte-Carlo sampling in Fig. 11 for both efficiency mean and standard deviation. It appears both efficiency mean and standard deviation are not changing significantly with the number of collocation points. It depends on the system that is studied and the order of the statistics that is required. In the present case, it appears that 2 collocation points are sufficient to calculate the mean and standard deviation. Small differences are observed between the results of the Monte-Carlo sampling and the stochastic collocation method but this is not surprising since neither the Monte-Carlo nor the collocation technique is perfect. The first would require an infinite number of samples and the second is based on an approximation of an integral quantity. As the difference sits around $10^{-3}\%$, it can be considered as negligible.

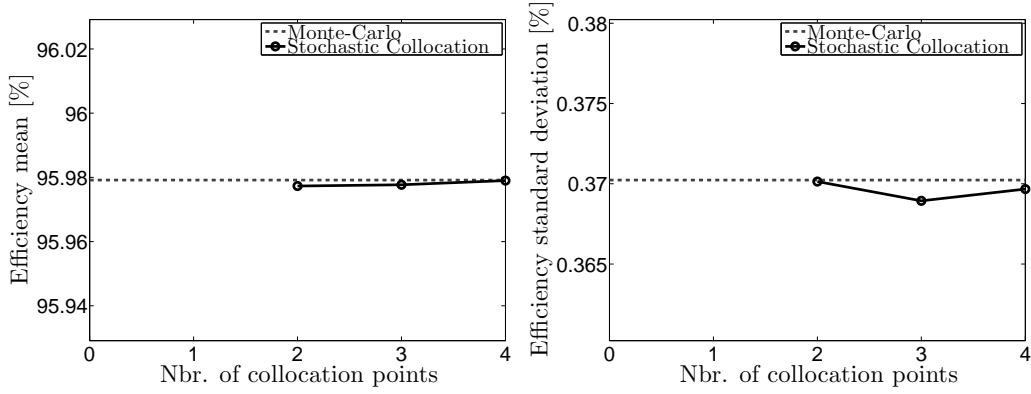


Figure 11: Efficiency mean and standard deviation in function of the number of collocation points ($D_{max} = 0.45$)

The same procedure has been applied to the optimum candidate at $D_{max} = 0.40$. Results are summarized in Table 2 for both optima at $D_{max} = 0.40$ and $D_{max} = 0.45$ using both Monte-Carlo sampling and stochastic collocation. The mean, the standard deviation and the 95% confidence interval $[\mu \pm 1.96\sigma]$ are indicated. The analysis of Table 2 reveals the importance of accurate and trustworthy correlations. The minimum standard deviation of the stage efficiency reaches 0.37%. Nowadays, compressor designers seek for 0.1% efficiency increase using three-dimensional blade design. Moreover, as seen in Fig. 10, it represents a 95% confidence interval that covers close to 1.5%. This study demonstrates that the meridional design may already bring a non-negligible amount of uncertainty due to the correlations.

		MONTE-CARLO SAMPLING		
		μ	σ	$[\mu \pm 1.96\sigma]$
$D_{max} = 0.40$	π [-]	1.2509	0.0012	$[1.2509 \pm 0.0024]$
	η [%]	95.56	0.44	$[95.56 \pm 0.86]$
$D_{max} = 0.45$	π [-]	1.2509	0.0011	$[1.2509 \pm 0.0022]$
	η [%]	95.98	0.37	$[95.98 \pm 0.73]$
		STOCHASTIC COLLOCATION		
		μ	σ	$[\mu \pm 1.96\sigma]$
$D_{max} = 0.40$	π [-]	1.2509	0.0012	$[1.2509 \pm 0.0024]$
	η [%]	95.55	0.43	$[95.55 \pm 0.84]$
$D_{max} = 0.45$	π [-]	1.2509	0.0011	$[1.2509 \pm 0.0022]$
	η [%]	95.98	0.37	$[95.98 \pm 0.73]$

Table 2: Monte-Carlo and stochastic collocations results using three uncertain parameters

OPTIMIZATION UNDER UNCERTAINTY

In the previous section, UQ techniques allowed to take into account the uncertainties of the loss correlations. Furthermore, the stochastic collocation method offers a very good estimate of the mean and the standard deviation of the output performance at affordable computational cost. In the case of ACPReDesign and because only the mean and the standard deviation were required, the previous section showed that 2 collocation points were sufficient. It is then realistic to consider solidity optimization where the pressure ratio, the average efficiency and its standard deviation are optimized.

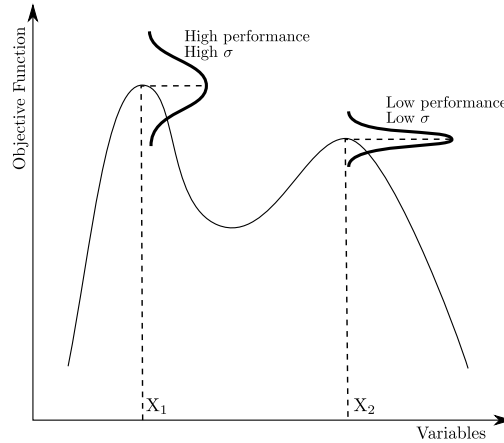


Figure 12: Illustration of the *robust design* problem on an arbitrary function presenting two extrema

Optimization under uncertainty is most of the time mentioned as the problem of *robust design*. This approach is not very common in compressor or turbine blade design, mainly due to high computational costs of CFD computations. Ideally, the aim is to look at a solution that is less sensitive to the uncertainties. In the case of Fig. 12, while a standard optimization, disregarding any fluctuation, would tend to the extremum in X_1 , a robust design may lead to an extremum in X_2 since it shows a lower standard deviation. However, the existence of such a robust optimum obviously depends on the system that is studied and the situation of Fig. 12 may not always occur. The main problems encountered in engineering when dealing with robust designs are exposed by Poloni et al. (2011).

Robust optimization has been performed involving 3 uncertain variables. The maximum diffusion factor has been set to 0.40 and 0.45. The pressure ratio, the efficiency and the efficiency standard deviation must be optimized. It is thus not anymore a single objective optimization. Since there are 3 uncertain parameters and 2 collocations points, each individual generated according to the DE algorithm requires 8 computations of ACPReDesign to obtain a mean and a variance. The rest of the optimization process remains unchanged. The pareto fronts are given in Fig. 13 in terms of pressure ratio versus efficiency. For the same number of population, the differences between a standard optimization and a robust optimization are very limited. At $D_{max} = 0.40$, the results are even identical. The convergence is slightly slower for $D_{max} = 0.45$ and bigger discrepancies are observed. However, the robust optimization definitely converges towards the pareto front of the standard optimization. Such results are very dependent on the solver that is studied, the chosen parametrization and the optimized parameters. It underlines that the response of ACPReDesign is very linear with respect to the uncertain inputs and that the situation depicted in Fig. 12 does not exist for the current test case. In other words, for the given problem of solidity optimization, the optimum solutions of Fig. 4 are also robust designs.

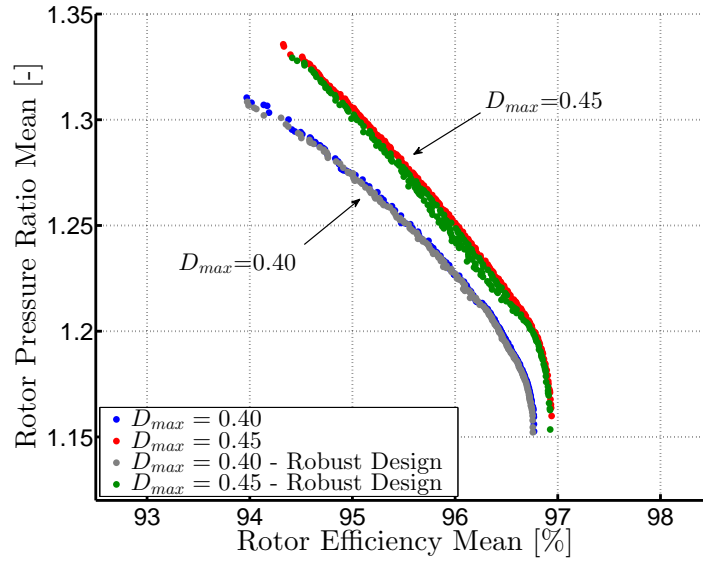


Figure 13: Comparison of Pareto fronts with or without considering uncertainties

CONCLUSION

A meridional solver relies on empirical correlations to obtain an estimate of the total pressure losses of a blade row. In the present investigation, the NISRE solver *ACPreDesign* is based on typical correlations originally established by Lieblein et al. However, empirical data often come with uncertainties that are usually neglected at the level of the meridional design.

This paper investigates the use of uncertainty quantification methods in the specific case of solidity optimization of a single rotor compressor. The study shows that both Monte-Carlo sampling as well as quadrature method compute uncertainty bands that cover 1.5% in efficiency. While, nowadays, 3D blade design optimization chases 0.1% improvements that are usually very difficult or impossible to validate experimentally, it represents a non-negligible amount of uncertainty that are disregarded by a standard deterministic approach. Such additional information may imply to increase the target efficiency according to the uncertainty band to guarantee a minimum efficiency above the design requirements.

Outside the framework of solidity optimizations, uncertainty quantification could be implemented at the level of meridional design to take into account various sources of epistemic uncertainties. For example, the use of UQ techniques may compensate the lack of knowledge related to the influence of the inlet boundary layer profile, the Reynolds number or the inlet turbulence intensity which can cause big variation in the meridional design performance in terms of pressure ratio, efficiency and mass-flow. Off-design correlations also represents a tremendous source of uncertainty that can radically affect the whole design. Finally, beyond the meridional design, non-deterministic CFD calculations may also play a crucial role in the management of turbulence modeling uncertainties.

The issue of the robust design was also addressed and, in the present case, the standard optimum design were already robust. The existence of a robust optimum strongly depends on the nature of the problem that is studied and, in many situations, an optimization under uncertainty may lead to the same solution as a standard optimization. Nevertheless, the study reveals the capability of performing meridional robust optimization which may represent a breakthrough in turbomachinery design.

REFERENCES

- H. F. Creveling and R. H. Carmody. Axial Flow Compressor Design Computer Programs Incorporating Full Radial Equilibrium - Part I: Flow Path and Radial Equilibrium of Energy Specified - Part II: Radial Distribution of Total Pressure and Flow Path or Axial Velocity Ratio Specified. Technical report, NASA, June 1968. NASA CR-54531 and NASA CR-54532.
- G. Iaccarino. Introduction to uncertainty representation and propagation. In *Uncertainty quantification in computational fluid dynamics*, RTO-AVT-VKI Lecture Series 2011/12 - AVT 193, Rhode-Saint-Genese, Belgium, October 2011.
- M. Joly, T. Verstraete, and G. Paniagua. Full Design of Highly Loaded Fan by Multi-Objective Optimization of Throughflow and High-Fidelity Aero-Mechanical Performance. In *Proceedings of ASME Turbo Expo 2012*, Copenhagen, Denmark, 2012. ASME Paper No. GT2012-69686.
- N. Lecerf, D. Jeannel, and A. Laude. A Robust Design Methodology for High-Pressure Compressor Throughflow Optimization. In *Proceedings of ASME Turbo Expo 2003*, Atlanta, Georgia, USA, 2003. ASME Paper No. GT2003-38264.
- S. Lieblein, F. C. Schwenk, and R. L. Broderick. Diffusion Factor for Estimating Losses and Limiting Blade Loadings in Axial-Flow Compressor Blade Elements. NACA Research Memorandum, Lewis Flight Propulsion Laboratory, Cleveland, Ohio, 1953. RME53D01.
- A. Panizza, D. T. Rubino, and L. Tapinassi. Efficient Uncertainty Quantification of Centrifugal Compressor Performance Using Polynomial Chaos. In *Proceedings of ASME Turbo Expo 2014*, Dusseldorf, Germany, 2014. ASME Paper No. GT2014-25081.
- C. Poloni, V. Pediroda, and L. Parussini. Optimization under uncertainty. In *Uncertainty quantification in computational fluid dynamics*, RTO-AVT-VKI Lecture Series 2011/12 - AVT 193, Rhode-Saint-Genese, Belgium, October 2011.
- K. Price and N. Storn. Differential Evolution. *Dr. Dobb's Journal*, pages 18–24, April 1997.
- W. H. Robbins, R. J. Jackson, and S. Lieblein. Aerodynamic design of axial-flow compressors - Chapter VII: Blade-element flow in annular cascades. NASA SP-36, 1965.
- J. Sans, J. Desset, G. Dell'Era, and J.-F. Brouckaert. Performance Testing of a Low-Pressure Compressor. In *The 10th European Turbomachinery Conference*, Finland, 2013.
- S. Teichel, T. Verstraete, and J. Seume. Optimized Preliminary Design of Compact Axial Compressors A Comparison of Two Design Tools. In *31st AIAA Applied Aerodynamics Conference*, San Diego, California, USA, 2013. AIAA-2013-2651.
- T. Verstraete. *Multidisciplinary Turbomachinery Component Optimization Considering Performance, Stress and Internal Heat Transfer*. PhD Thesis, von Karman Institute for Fluid Dynamics - Universiteit Gent, Rhodes-Saint-Genese, Belgium, 2008.
- T. Verstraete. CADO: a Computer Aided Design and Optimization Tool for Turbomachinery Applications. In *2nd International Conference on Engineering Optimization*, Lisbon, Portugal, 2010.